Hydration of Sodium, Potassium, and Chloride Ions in Solution and the Concept of Structure Maker/Breaker

R. Mancinelli, A. Botti, F. Bruni, and M. A. Ricci*

Dipartimento di Fisica "E. Amaldi", Università degli Studi "Roma Tre", Via della Vasca Navale 84, 00146 Roma, Italy

A. K. Soper†

ISIS Facility, Rutherford Appleton Laboratory, Harwell Science and Innovation Campus, Didcot, Oxfordshire, OX11 0QX, United Kingdom

Received: July 26, 2007; In Final Form: September 17, 2007

Neutron diffraction data with hydrogen isotope substitution on aqueous solutions of NaCl and KCl at concentrations ranging from high dilution to near-saturation are analyzed using the Empirical Potential Structure Refinement technique. Information on both the ion hydration shells and the microscopic structure of the solvent is extracted. Apart from obvious effects due to the different radii of the three ions investigated, it is found that water molecules in the hydration shell of K^+ are orientationally more disordered than those hydrating a Na^+ ion and are inclined to orient their dipole moments tangentially to the hydration sphere. Cl^- ions form instead hydrogen-bonded bridges with water molecules and are readily accommodated into the H-bond network of water. The results are used to show that concepts such as structure maker/breaker, largely based on thermodynamic data, are not helpful in understanding how these ions interact with water at the molecular level.

I. Introduction

The viscosity of salt solutions,[1] the behavior of ionic mobility as a function of ionic radius,[2] the ionic selectivity of membrane channels,[3] and the sensitivity of protein salting-in or -out to different ions[4] are macroscopic examples of the competing interactions between dissolved ions, water, and larger molecular units in solution. They suggest that the extent of influence of ions on the microscopic structure of water (as a solvent) and the structure of the ion hydration shell is highly specific to individual ions. Given the current vibrant debate about the mechanism by which membrane proteins can be highly selective about distinguishing between sodium and potassium ions, along with the known electrostrictive effects,[5,6] many of these phenomena are waiting for a microscopic interpretation, beyond the simplistic definition of ions as structure makers/breakers[7] or cosmotrope/chaotrope.[8] In particular, it should be noted that the classification of an ion as a structure maker or structure breaker can also depend on its concentration. The experimental determination of the microscopic structure of aqueous salt solutions is the first step toward a detailed understanding of these properties.

A number of recent papers[9−13] have highlighted how modern neutron diffraction techniques and the associated data interpretation methods can be used to explore the microscopic structure of acid, alkali, and monovalent salt solutions. These follow the much earlier work of Enderby and co-workers[14] using neutron diffraction with isotope substitution (NDIS) on the dissolved ions and the subsequent extensive tabulations of ion water coordination numbers and distances from a variety of sources.[15,16]

In all of these cases, the ions in question have the ability to strongly reorient the local water structure. This reorientation means that a single diffraction experiment is not sufficient to define the structure, since the measured differential cross section is a weighted sum of contributions from the Fourier transform of several correlation functions averaged over molecular orientations.[14] The use of hydrogen/deuterium substitution in such cases helps identify the extent to which water structure is modified in the presence of ions,[17] because the water hydrogen atoms carry the necessary orientational information into the diffraction experiment.[18]

In this paper, after a short description of the neutron diffraction and empirical potential structure refinement methods (EPSR),[19,20] we report the results of a diffraction experiment performed on aqueous solutions of NaCl and KCl as a function of the salt concentration, using hydrogen isotope substitution to separate out the hydrogen−hydrogen and hydrogen−other correlations from the other−other correlations. A previous paper has described the overall effect of the ions on water structure.[17] Here, we concentrate on the ion hydration and ion pairing and discuss these in terms of structure making and structure breaking concepts and the differences between sodium and potassium ion hydration.

II. Neutron Diffraction Theory

When a salt, say Z^+A^-, is dissolved in water, at least 10 site−site radial distribution functions (s-sRDF) are required, namely,[21] $g_{OO}(r)$, $g_{OH}(r)$, $g_{HH}(r)$, $g_{ZO}(r)$, $g_{ZH}(r)$, $g_{AO}(r)$, $g_{AH}(r)$, $g_{ZA}(r)$, $g_{ZZ}(r)$, $g_{AA}(r)$.[14] The first three functions contain information on the water−water correlations in the presence of the solute; the following four functions describe the cation and anion hydration structures respectively, and the last three

* Corresponding author. E-mail: riccim@fis.uniroma3.it.
† Department of Physics and Astronomy, University College London, Gower Street, London WC1E 6BT, U.K.

10.1021/jp075913v CCC: $37.00
Published on Web 11/08/2007

TABLE 1: Weights $w_{\alpha\beta} = c_\alpha c_\beta b_\alpha b_\beta (2 - \delta_{\alpha\beta})$ of the Individual PSF in the DCS of Solutions of NaCl in D_2O at Two Concentrations, Given as "Number of Solute Molecules: Number of Solvent Molecules"; c_α is the Atomic Fraction, and b_α the Neutron Coherent Scattering Length[24] of the α Species

1:10	O	D	Na	Cl
O	3.326	15.30	0.3783	0.9981
D		17.58	0.8698	2.295
Na			0.01076	0.05676
Cl				0.07487
1:83	**O**	**D**	**Na**	**Cl**
O	3.682	16.93	0.0555	0.01464
D		19.46	0.1276	0.3367
Na			0.0002	0.00110
Cl				0.00146

describe the ion−ion correlations. These latter functions are of interest in particular at high solute concentration, when ion pairing may occur. It is worth stressing here that the water−water correlations are used to describe water structure in the presence of ions, while the ion−water RDFs describe the hydration structure of each ion. Although they are linked, given that the correlation of water molecules around an ion must clearly affect the correlation between water molecules, formally, they are distinct, in that the water−water correlations can be compared directly with the same quantities in pure water, whereas the ion−water (and ion−ion) correlations cannot. It is to be noted that the ion−hydration structure is frequently referred to as the "water structure" in solution, but formally this is incorrect.

Each RDF is the Fourier transform of a partial structure factor (PSF), $S_{\alpha\beta}$, which is embedded in the measured neutron interference differential cross section (IDCS):

$$F(Q) = \sum_{\alpha} \sum_{\beta \geq \alpha} w_{\alpha\beta} S_{\alpha\beta}(Q) \tag{1}$$

where

$$S_{\alpha\beta}(Q) = 4\pi\rho \int_0^\infty r^2 (g_{\alpha\beta}(r) - 1) \frac{\sin(Qr)}{(Qr)} \, dr \tag{2}$$

and ρ is the atomic number density of the solution in question.

The difficulty in interpreting the diffraction pattern in terms of water−water, ion−water, and ion−ion correlations can be appreciated looking at Table 1, where the weights, $w_{\alpha\beta}$, of the individual PSF in eq 1 are reported for two NaCl solutions as an example. It is apparent that the IDCS is dominated by the S_{OD} and S_{DD} signals at all solute concentrations and that the information about the solute−solute and solute−water correlations becomes increasingly buried as the solute concentration decreases. Moreover, the S_{OD} and S_{DD} functions contain information about the local hydrogen bonding and orientational order between water molecules, but the more weakly weighted S_{OO} function is the most informative about medium range order and is sensitive to temperature and pressure changes.[22,23]

The $F(Q)$ function is only accessible from a diffraction experiment after reduction of the raw data to absolute differential cross section (DCS) using vanadium calibration measurements, removal of the single atom scattering, and making corrections for attenuation, multiple scattering, and inelastic scattering.[25,26] All of these corrections can in principle introduce systematic artifacts to the final extracted IDCS. On the other hand, neutrons have the unique characteristic of being sensitive to the isotopic state of the nuclei, through the scattering length b_α. Thus, changing the isotopic composition of the solution gives access to a different diffraction pattern. Under the assumption that the microscopic structure of the system is not affected by the isotopic status of the nuclei, this yields more detailed structural information on the sample, provided that isotopes with sufficiently different scattering lengths are available.

For the particular case of salt solutions, since $b_H = -3.742$ fm and $b_D = 6.674$ fm, the isotopic H/D substitution (IHDS)[27] technique can be applied to the solvent. When at least three experiments on different isotopic mixtures are performed, one can get three composite partial structure factors (CPSF), namely, S_{HH}, S_{XH}, and S_{XX}. By rearranging the terms of the linear combination in eq 1, each measured DCS can be written as:

$$F(Q) = c_X^2 \langle b_X \rangle^2 S_{XX}(Q) + 2 c_X c_H \langle b_X \rangle \langle b_H \rangle S_{XH}(Q) + c_H^2 \langle b_H \rangle^2 S_{HH}(Q) \tag{3}$$

where $c_X = c_O + c_Z + c_A$; $c_H = 1 - c_X$; $\langle b_X \rangle = [c_O b_O + c_Z b_Z + c_A b_A]/c_X$; and $\langle b_H \rangle$ is the scattering length of hydrogen/deuterium or a combination of the two, according to the isotopic substitution performed. The three CPSF are then obtained by linear combination of the measured IDCS, and $S_{HH}(Q)$ gives directly the radial distribution function between the water hydrogen atoms, while the other terms are:

$$S_{XX}(Q) = \frac{\sum_{\alpha,\beta \neq H} c_\alpha c_\beta b_\alpha b_\beta S_{\alpha\beta}(Q)}{(c_X \langle b_X \rangle)^2}$$

$$S_{XH}(Q) = \frac{\sum_{\alpha \neq H} c_\alpha b_\alpha S_{\alpha H}(Q)}{(c_X \langle b_X \rangle)} \tag{4}$$

At sufficiently low salt concentration, $S_{XX}(Q)$ and $S_{XH}(Q)$ are dominated by the water−water correlations, but one must always be cautious to include the ion−water correlations (and to a lesser extent for $S_{XX}(Q)$ the ion−ion correlations) before interpreting the RDF of these functions in terms of water structure.

III. Empirical Potential Structure Refinement (EPSR)

To interpret these functions, the traditional method was to Fourier transform the diffraction data to r space and compare with computer simulation.[27] On the other hand, computer simulation techniques are now widely available, and specialized codes for generating a three-dimensional structural model of a disordered sample consistent with a set of diffraction data have been developed. These codes, namely, reverse Monte Carlo (RMC)[28,29] and empirical potential structure refinement (EPSR),[19,20] are similar in principle to those routinely used in crystallography in that they attempt to systematically refine a structural model of the diffraction data to give overall agreement with those data. They can also help to identify any systematic bias that may affect one or more datasets. These systematic effects, which can be present in all diffraction experiments to a greater or lesser extent, are much more problematic for a liquids experiment compared with the corresponding crystalline experiment, since the diffraction signal for a liquid is typically 10 to 100 times weaker than that for a crystal. Systematic effects are identified when features in the data not compatible with physical configurations of molecules are found.

The EPSR method builds a simulation box with the same density and composition as the real sample. It does this by means

TABLE 2: Details of the Simulation Boxes: L Is the Box Length; N_w Is the Number of Water Molecules; and N_s Is the Number of ZA Couples

	c	L (Å)	N_w	N_s
NaCl	1:10	25.95	500	50
	1:17	25.18	500	30
	1:40	25.17	520	13
	1:83	24.74	500	6
KCl	1:13	25.79	578	39
	1:17	25.45	500	30
	1:40	25.30	520	13
	1:83	24.80	500	6

of a reference interaction potential, U_{ref}, which incorporates the distinctive characteristics of the system in question (such as, for instance, the presence of H bonds) and is used to seed the Monte Carlo (MC) simulation. Once it has reached equilibrium, a perturbation to the reference potential, called the empirical potential, derived directly from the diffraction data, is introduced and used to drive the simulated diffraction patterns as close as possible to the measured data. Since diffraction data are derived directly from the pair correlation function, this empirical potential is by definition purely pairwise additive. The Monte Carlo simulation proceeds using both the reference potential and the empirical potential to accept or reject moves, and the empirical potential is adjusted iteratively until the fit to the data cannot be improved further. At this point, the Monte Carlo production run begins and molecular configurations are accumulated and used to directly calculate the individual s-sRDF. As a consequence, the statistical noise on each function depends on both the number of recorded configurations and the concentration of relevant atomic pairs and decreases in proportion to the number of recorded configurations.

The EPSR code can currently be used to analyze IDCS, with or without H/D substitution, CPSF data, data from first or second order difference experiments, as well as data from X-ray diffraction experiments if available. References 19 and 20 give full details of how this is achieved.

IV. Experimental Details and Data Analysis

IHDS experiments have been performed on NaCl and KCl aqueous solutes, at a salt concentration ranging from 1 solute per 83 water molecules to 1 solute per 10 (NaCl) or 13 (KCl) water molecules, at standard temperature and pressure ($T = 298$ K, $p = 1$ bar). Measurements have been carried out at the SANDALS[30] diffractometer, installed at the ISIS Facility[31] (U.K.). In addition to the measurement of the samples, data were collected on the background scattering, empty containers and vanadium sample, used for putting the data on an absolute scale of scattering cross section.

Diffraction data have been analyzed by using the ATLAS routines, which perform corrections for multiple scattering, absorption, and inelasticity effects, along with subtraction of the scattering from the sample container and data reduction to an absolute scale.[26] At each concentration, three solutions with different H/D content have been prepared: one fully deuteriated, one fully protiated, and an equimolar mixture of the two. The outputs of the ATLAS routines are the three CPSF defined in eqs 3 and 4. These have been used as input of the EPSR routine.

At each salt concentration, a simulation box has been prepared according to Table 2, in order to match the experimental density[32] and composition of the samples. The simple point charge/extended (SPC/E)[33] model has been used as reference potential for water; the ion sites have been modeled as Lennard-Jones centers (see Table 3 for the parameters), plus charges,

TABLE 3: Parameters of the Reference Potential

	ϵ (kJ/mol)	σ (Å)	M	q (e)
O	0.65	3.166	16	−0.8476
H	0	0	2	0.4238
Cl	0.566	4.191	36	−1
Na	0.5144	2.29	23	1
K	0.5144	2.94	40	1

with the parameters adjusted to give the expected ion water distances.[15,16]

The typical quality of a fit is shown in Figure 1 at one of the measured NaCl solutions. Figure 2 reports the fits of the data at all salt concentration in the case of NaCl. Strong modifications of the diffraction pattern are visible, in particular, in the S_{XX} CPSF, which is dominated by the OO contribution. At low salt concentration, this shows a double structured first peak, with maxima at about 2.2 Å^{-1} and 2.9 Å^{-1}, indicative of the presence of a tetrahedral network of water molecules, followed by a minimum at about 3.7 Å^{-1}. As the salt concentration increases, the intensity of the first structure increases, while that of the second structure decreases and the minimum moves to shorter wave vectors, suggesting the occurrence of distortions of the tetrahedral network. The first peak of the S_{XH} CPSF, which is dominated by the OH contribution, becomes sharper and moves to larger wave vectors with increasing salt concentration, while the small peak at about 4 Å^{-1}, which is characteristic of water in the liquid phase, moves toward the first one and becomes broader: this suggests that changes are expected in the hydrogen bond peaks. As far as the S_{HH} CPSF is concerned, the major changes are visible in the second peak at about 3.45 Å^{-1}, which becomes progressively less intense. Since this CPSF contains information only on the water−water correlations, this finding confirms that the structural arrangement of water molecules is changing because of the presence of solutes. The same trend is observed in the data relative to the KCl solutions.

It is worth pointing out that the fit of the experimental data of the quality shown in Figure 1 is usually achieved allowing very small perturbation to the reference potential (see Figure 3 as far as the OO pair additive contribution is concerned). We notice also that the shape and intensity of the empirical potential is similar at all salt concentrations, but the highest one requires a deepest well at short distances (see the inset of Figure 3).

V. Cation Hydration Shell

For both Na and K, the hydration shell is very weakly sensible to the concentration and in particular the position of the first peak of both $g_{ZO}(r)$ and $g_{ZH}(r)$ (Table 4) does not change, while the peak intensity changes and the number of hydration water molecules decreases from 5.3 to 4.5 in the case of Na and from

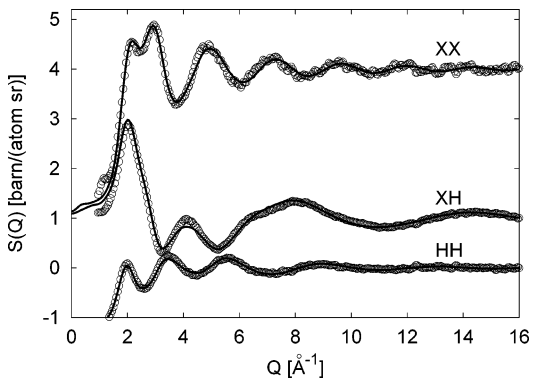

Figure 1. CPSF functions for the 1:83 NaCl solution: circles and solid lines represent the experimental data and fits, respectively.

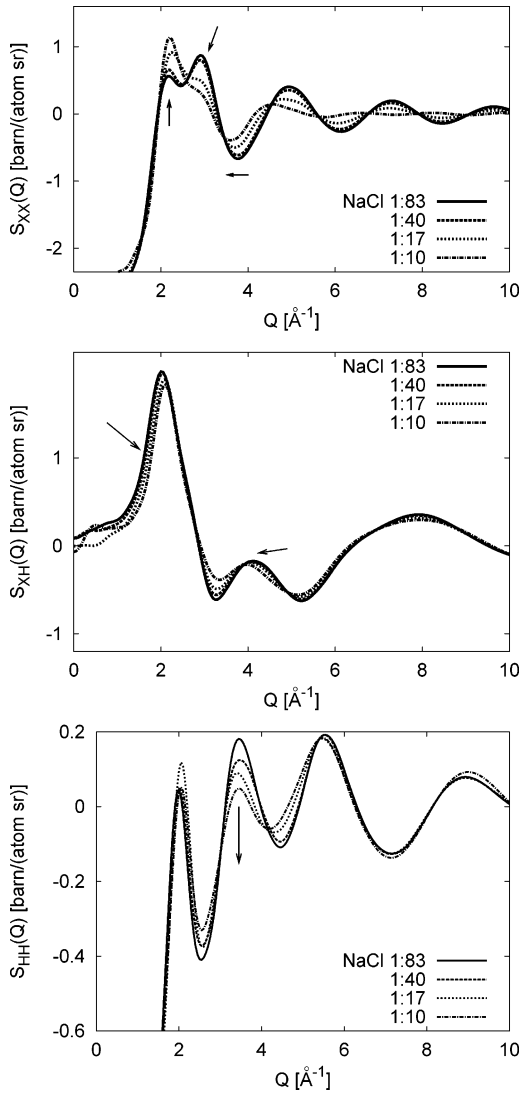

Figure 2. $S_{XX}(Q)$ (top), $S_{XH}(Q)$ (middle), and $S_{HH}(Q)$ (bottom) functions for all measured NaCl solutions. The arrows point to the modifications of the structure factors with concentration.

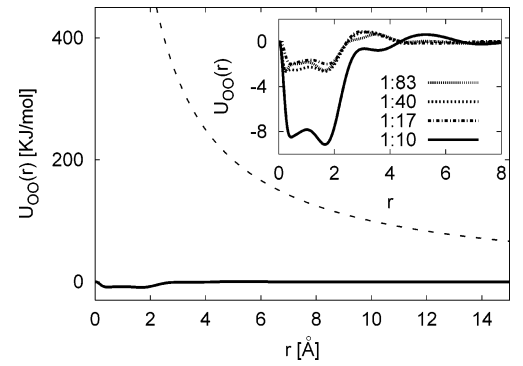

Figure 3. Reference potential (dashed line) for the OO pair (the same for all concentrations), compared with the largest empirical correction (solid line), which occurs for the 1:10 NaCl solution. In the inset, the empirical correction is reported at all studied NaCl concentration.

6.0 to 4.8 for the larger K ion, respectively. Incidentally, the first peak positions and coordination numbers (Table 5) compare well with previous findings from both experiments and simulations.[34] Instead we remind that in the case of NaOH and KOH solutions the cation−water oxygen distances were systematically larger and concentration dependent.[10]

TABLE 4: Positions of the First Peak of the Individual Radial Distribution Functions, r_{ij}^I, Where Data Are Reported in Å, along with Their Standard Deviation (in Parenthesis), at the Two Extreme Concentrations for Both NaCl and KCl Solutions

NaCl	1:83	1:11
OO	2.75 (0.15)	2.76 (0.21)
NaO	2.34 (0.14)	2.34 (0.14)
ClO	3.16 (0.11)	3.16 (0.16)
NaH	2.97 (0.12)	2.98 (0.05)
ClH	2.19 (0.16)	2.20 (0.06)
KCl	**1:83**	**1:13**
OO	2.75 (0.16)	2.77 (0.17)
KO	2.65 (0.18)	2.65 (0.18)
ClO	3.14 (0.17)	3.15 (0.20)
KH	3.25 (0.22)	3.27 (0.16)
ClH	2.18 (0.04)	2.18 (0.09)

TABLE 5: Ion−Water Coordination Numbers (the Uncertainties Are Reported within Parenthesis), along with the *r*-Range Used in the Integration

NaCl	NaO	NaH	ClO	ClH
r-range (Å)	2.0−3.2	2.0−3.7	2.6−3.8	1.5−2.9
1:83	5.3 (0.8)	13.9 (1.0)	6.9 (1.0)	6.0 (1.1)
1:40	5.1 (0.9)	13.7 (2.4)	6.8 (1.1)	5.9 (1.1)
1:17	4.6 (1.4)	12.1 (1.9)	6.6 (1.3)	5.3 (1.5)
1:10	4.5 (1.4)	11.6 (2.4)	6.3 (1.3)	5.3 (1.5)
KCl	**KO**	**KH**	**ClO**	**ClH**
r-range (Å)	2.2−3.45	2.0−4.1	2.6−3.8	1.5−2.9
1:83	6.0 (1.2)	16.5 (2.0)	7.0 (1.1)	6.1 (1.0)
1:40	6.1 (1.2)	16.9 (2.0)	6.8 (1.1)	6.1 (1.1)
1:17	5.5 (1.1)	16.9 (1.9)	6.3 (1.3)	5.4 (1.4)
1:13	4.8 (1.6)	15.0 (2.9)	5.7 (1.5)	4.9 (1.5)

Up to the recent past,[8] the observation that $r_{KO}^I > r_{NaO}^I$ along with a lower peak intensity has been taken as a signature of the structure breaking character of K compared with Na. This point deserves a deeper discussion. First of all, the lower intensity of the first peak of a RDF is not a signature of a weaker binding, because this function does not measure the strength of the interaction between two atomic sites. On the contrary, it gives information on the average number of neighbor atoms within a sphere of radius R, through the integral $n(R) = \int_0^R 4\pi r^2 g(r)\,dr$. In this specific case, the first peak of $g_{KO}(r)$ is less intense, but being shifted to larger distances compared with that of $g_{NaO}(r)$ gives about the same coordination number as for Na. Second, the different position of the first peak is a trivial consequence of the different ionic size. The availability of a simulation box reproducing the experimental data provides instead more solid information.

The comparison of the first peak positions of the cation−water oxygen and cation−water hydrogen ss-RDF suggests that the angle formed between the water dipole and the Z−O director has a broader distribution in the case of K compared with Na, as confirmed in Figure 4. These findings are mirrored in Figure 5, where the $g_{ZO}(r)$ and $g_{ZH}(r)$ functions of the 1:83 solutions are reported after scaling of the abscissa relative to r_{ZO}^I, in order to uncover differences between the two hydration shells apart from the trivial ionic dimensions. In this plot, the first peak of the $g_{KH}(r)$ and the second of the $g_{KO}(r)$ come to shorter distances compared with their analogues for the NaCl solutions; moreover, the hydration shell of the Na ion is better defined than that of K. These findings reveal that water molecules in the hydration shell of the K ions, at variance with those hydrating a Na ion, are orientationally more disordered and tend to bring their dipole moments more tangential to the hydration

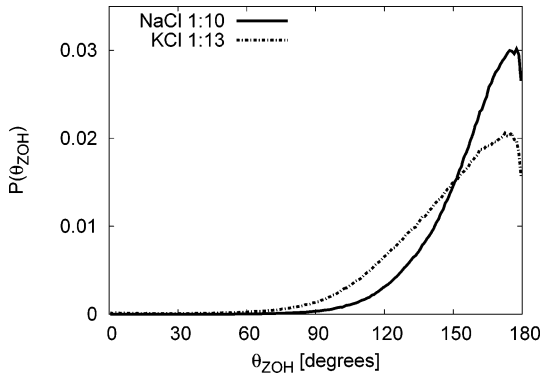

Figure 4. Distribution function of the angle formed between the cation-water oxygen director and the dipole of water molecules within the cation hydration shell in the case of 1:40 solution of NaCl (solid line) and KCl (dashed line).

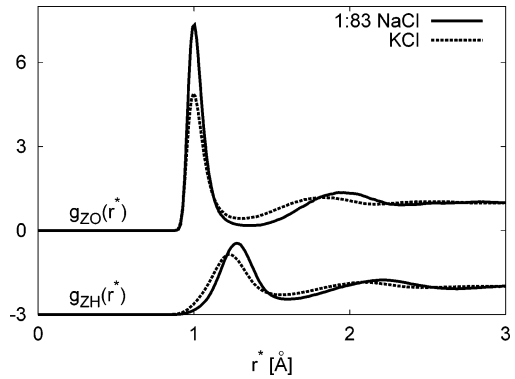

Figure 5. $g_{ZO}(r)$ and $g_{ZH}(r)$ for the 1:83 solutions of NaCl (solid line) and KCl (dashed line) as a function of a reduced abscissa $r^* = r/r^I_{ZO}$.

shell. As a consequence, the second hydration shell can move to r^* distances shorter than 2. We notice also that the ratio of the coordination numbers reported in the II and III column of Table 5 is ∼2.6 for NaCl and changes from ∼2.8 to ∼3.1 in the case of KCl, thus confirming a difference in the orientational correlations of water molecules around the two cations. Moreover, the looser first minimum of the $g_{KO}(r)$ is reminiscent of faster exchange of water molecules between the first and the second shell.[35,36] These conclusions are qualitatively similar to those found in the case of hydroxide solutions,[10] although in that case a larger concentration dependence was found.

VI. Chloride Hydration Shell

The chloride hydration shell, Figure 6 and Table 4, is substantially independent of the counterion at low salt concentration, while small differences of peak intensities and position of the first minimum and second peak show up as the salt concentration increases. These changes bring only small but systematic changes to the number of molecules participating in the hydration shell of the anion, which decreases from about 6.1 ± 1.1 to 5.6 ± 1.6 water molecules as the salt concentration increases: this supports the claim for the independence of the counterion hydration on concentration reported in ref 34.

The positions of the first peak of the $g_{ClO}(r)$ and $g_{ClH}(r)$ differ by about 1 Å, and the first peak of the $g_{ClH}(r)$ is sharp enough in all solutions to suggest that the hydrogens form almost linear bridges between the chloride and the oxygens. This inference is confirmed by the isosurfaces of probability of finding a chloride ion within the first neighboring shell of a water molecule sitting at the origin of the reference frame: these are actually very close to those found for two acceptor water

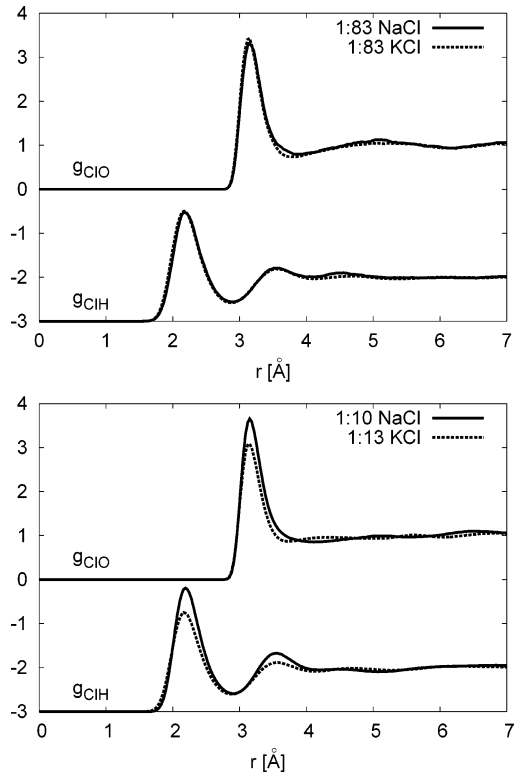

Figure 6. Chloride−water RDF at the highest (top) and lowest (bottom) salt concentrations, for NaCl solutions (solid line) and KCl ones (dashed line).

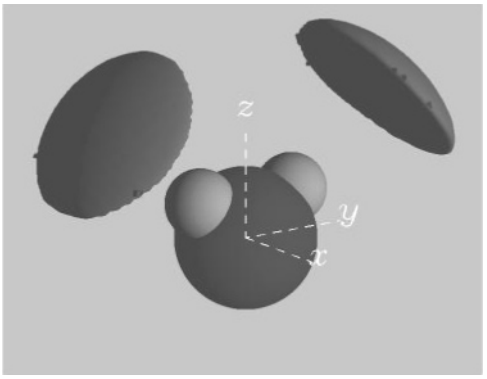

Figure 7. Isosurfaces of probability of finding a Cl ion first neighbor of a water molecule, placed at the origin of the reference frame. The horizontal dimension of the plot is 4 Å and the contrast level used for the isosurphaces is 0.30.

oxygens facing the hydrogen sites of the first molecule (see Figure 7), albeit at a slightly longer distance.[38]

On the other hand, the distribution of the H−Cl−H angle reported in Figure 8 is peaked at about 70°, as opposed to the 104° characteristic tetrahedral coordination, indicating a structure similar to distorted octahedral coordination. We notice also that the ClO coordination number systematically exceeds the ClH coordination number (see Table 5), suggesting the presence of an interstitial water molecule in the hydration shell, that is, a water molecule which does not form a hydrogen bridge with the chloride. This is confirmed by the distribution of the O−Cl−O angles, which exceeds that of the H−Cl−H angles around 45° (data not shown).

The comparison with the chloride hydration shell determined in a concentrated HCl solution[11] confirms the independence on the counterion.

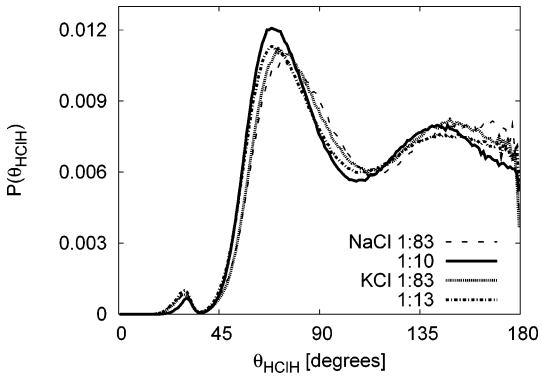

Figure 8. Distribution functions of the H−Cl−H angles at the extreme concentrations for both salts solutions.

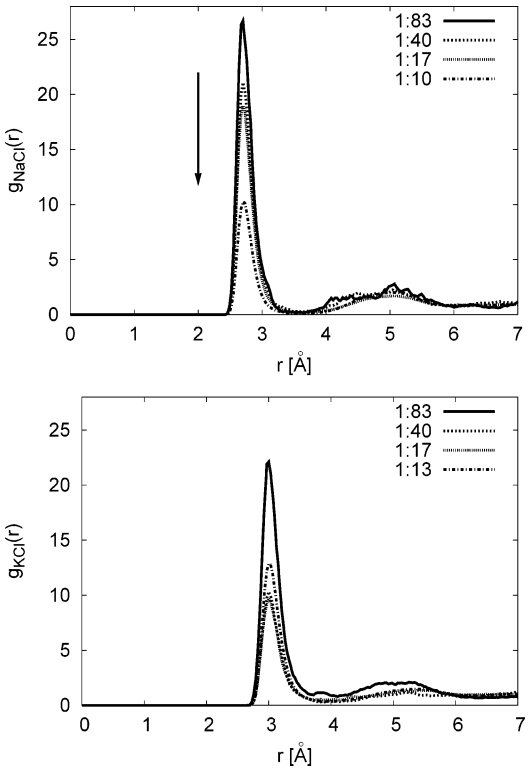

Figure 9. Cation−anion RDF for NaCl (top) and KCl (bottom) solutions.

VII. Ion Pairing

Although there is, as discussed previously, no direct information in the neutron experiment on the extent of ion−ion interactions (because of its weak contribution to the diffraction pattern, Table 1), there is information in the EPSR simulation about such correlations. The correlations reported here therefore are based on a model of the solution which is consistent with the diffraction data and with other physical constraints such as the opposite charges on cation and anion.

The occurrence of contact ion pairing in solution is expected to be a function of the salt concentration, and indeed, the number of cation−anion contacts regularly increases from about 0.3 ± 0.5 to 0.9 ± 1.0 for Na−Cl and from 0.5 ± 0.6 to 1.3 ± 1.1 for K−Cl. Although the uncertainty on these numbers is quite high, nevertheless, the difference between the two solutions may mirror the lower solubility of KCl compared with NaCl.[39] The first peak is located at ∼2.75 Å for $g_{NaCl}(r)$ and at ∼3.0 Å for $g_{KCl}(r)$ (see Figure 9); again, this difference depends on the different ionic radius of the two cations. These latter distances

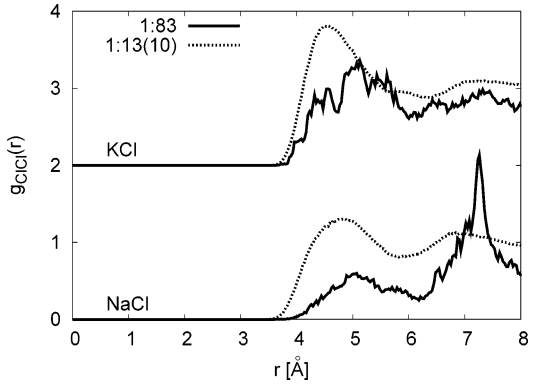

Figure 10. Anion−anion RDF for KCl (top) and NaCl (bottom) at the two extreme concentrations, high (dotted) and low (solid).

indicate contact ion pairs at all concentrations but especially at the highest concentrations, given that the Cl−O distance in solution is about 3.2 Å. Therefore, it seems likely that, especially at higher salt concentrations, there will be counterions on the inside of the chloride hydration shell in solution, a fact that was not explicitly included in the early analysis of FOD experiments.[40] On the other hand, these distances mean that the ion pairs are outside or at least on the outer edge of the cation−water hydration shell in both cases (Table 4). Hence, we find an interesting asymmetry between the hydration of cation and that of anion, namely, the chloride hydration shell is likely to contain contact ion pairs, while these are unlikely within the cation hydration shell.

The $g_{ClCl}(r)$ function is reported in Figure 10 at the two extreme concentrations for both solutions. These functions present two maxima within a distance of 8 Å, and the first moves to shorter distances and becomes more intense as the salt concentration increases: these changes are indeed best visible in the case of NaCl. Also the cation−cation RDF present two maxima within the 0−8 Å range, and again in this case, the first one is very broad at low salt concentration and becomes more intense and better defined at the highest concentration. Within the experimental uncertainty, at all concentrations, the number of cation−cation and anion−anion contacts is below 1. Moreover, the latter is consistent with one or two solvent molecules in between (see Figure 10).

VIII. Discussion

The analysis of a series of IHDS experiments on NaCl and KCl at concentrations ranging from saturation to high dilution, performed within the EPSR framework, has allowed us to investigate the microscopic structure of models of these solutions which are consistent with the diffraction data. Previously, we reported on the effects of ions on the water structure itself[17] where it was shown that as the concentration increases the water structure itself behaves in an analogous manner to pure water under pressure, and this effect can be used to characterize the water structure in solution in terms of an equivalent pressure.[9−11,41]

What is the origin of this pressure-like effect? The present analysis may be giving some clues. In particular, we see that both sodium and potassium ions strongly coordinate water molecules with the oxygen atom pointing toward the ion and hydrogen atoms pointing away (Figure 5), although there is a strong disorder in the angle the water molecule's dipole moment makes with the ion−water axis (Figure 4). This means that the hydration of both ions must involve significant disruption to the water network, with highly bent or broken hydrogen bonds. Just as occurs in pure water with increased external pressure,

this bond bending is achieved not by disrupting the immediate tetrahedral-like coordination shell of a water molecule, but by modifying the second shell, which is pulled inward under pressure and under the influence of dissolved ions. The coordination number of both ions is approximately 6 at all concentrations. The ion−water distances are approximately 2.34 and 2.65 Å for sodium and potassium, respectively (Table 4), which means with roughly octahedral coordination, the mean separation of water molecules within this hydration shell is ∼3.3 and ∼3.7 Å respectively. These distances are much longer than the position of the first peak in $g_{OO}(r)$ but shorter than the position of the second peak in the same function for pure water, which occurs at ∼4.5 Å.

This, no doubt, explains the inward movement of the second peak $g_{OO}(r)$ with increasing salt concentration, but does not explain how the same movement is observed, albeit to a lesser extent, in the water outside the first hydration shell of both anion and cation.[17] The only conclusion can be that the effect of relatively small, positively charged ions is to affect the water structure beyond the first hydration shell. The same conclusion was made in a recent study of potassium halides in solution.[42] Hence, the notion of "electrostriction" to describe the effect of these ions on local water structure appears to be very pertinent here: the effect of such ions on water structure is unquestionably to compress the local water order.

On the other hand, the chloride ion appears to be able to fit into the structure of water without a large perturbation. There is only one hydrogen atom on each water molecule pointing toward the chloride ion (see Figure 8), leaving the remaining hydrogen atom and two lone pair electrons available for bonding to other water molecules or ions. The Cl−O distance is ∼3.2 Å which means, although there is sixfold coordination of the ion, the separation of water molecules in the hydration shell of Cl is ∼4.5 Å, which is closely similar to the second neighbor distance in pure water. Therefore, chloride can apparently fit into the water structure relatively easily without a large perturbation to the water structure. However, included in that hydration shell will be up to one cation, while the cation itself will have the chloride only on the periphery of its hydration shell (especially for sodium, where the sodium−water distance is much shorter than the sodium−chloride contact distance).

The subtle differences between cation's hydration shells may be a significant clue as to how it is possible for membrane channel proteins to distinguish between the different ions in solution and let some pass and not others.

In terms of the labeling of ions as structure makers and structure breakers, we can see here that the present results do not support the use of these concepts at the molecular scale. Both sodium and potassium have a significant structure breaking effect on water structure, while chloride appears relatively inefficient in this regard. On the other hand, the water attached to sodium is clearly more tightly coordinated than that attached to potassium, so in terms of the water attached to these ions, sodium could be regarded as the stronger (local) structure maker, even though relative to the water structure it is clearly a structure breaker.

The clue to the properties of these cations in solution is almost certainly wound up in the type of anion that is present. For example, for the hydroxides in solution,[10] it was found that potassium had a greater effect on water structure than sodium. In the present instance, the distinction between the ions is not so clear-cut, since the near saturated solutions used here correspond to different concentrations of ions (1:10 for NaCl, 1:13 for KCl). Nonetheless, by reviewing the earlier analysis,[17] one gets the impression that it is sodium that has the bigger impact on water structure in this case. The difference between the hydroxide solutions and the present case is the chloride counterion. For NaOH and KOH, the counterion will appear inside the first hydration of the cations.[9,10] Since the anion in these cases, due to its small size, will itself be involved in a significant amount of water structure breaking, it is possible the close proximity of OH to Na will to some extent mask the effect of the bare ions on the local water order, making sodium in these cases less effective at disrupting water structure than potassium, where the cation−anion distance is larger and the corresponding masking is less pronounced. In the present cases of NaCl and KCl, it is possible the reverse happens, namely, the counterion is outside the immediate hydration shell of the cations, so that sodium is more effective at disrupting water structure than potassium, and in any case chloride appears rather weak at disrupting water structure. Either way, it is very clear that it is important to consider the nature of the counterion when trying to understand the structural properties of these ions in solution. It is for these reasons that we believe the notions of structure maker and structure breaker, or cosmotrope versus chaotrope, which are largely derived to represent macroscopic properties are not relevant when discussing the microscopic impact of these ions on water structure.

IX. Conclusions

The availability of molecular configurations compatible with a set of experimental diffraction data, as well as being based on the known physics of these solutions, has allowed us to probe some of the questions that arise when discussing ions in water. Not only is it possible to identify the individual site−site radial distribution functions, but also it is possible to discuss the overall structure in terms of bond angle distributions and spatial density functions. In particular, we have shown previously that the ions can affect the structure of water well outside the first hydration shell.[17]

The results of the present analysis along with those of similar studies performed on other electrolyte solutions[9−11,41] bring to light the weakness and contradictions of the classical concepts of "structure maker/breaker". As a matter of fact, if we look at the cation hydration shell, the orientational distribution of water molecules is broader around a K ion compared with a Na one. Only on the basis of this observation, one could infer a "structure breaker" character of K as opposed to the "structure maker" character of Na. On the contrary, if we look at the effect of the solute on the water−water correlations, the greater distortions compared to pure bulk water are observed in the presence of NaCl, in contrast to previous inferences based on the hydroxide solutions and highlighting the role of the counterion in affecting the water structure. However, the maximum concentrations of NaCl and KCl achieved in the present work were not the same, so it is not totally clear from the present results which ion is the greater water structure breaker. Certainly, both ions produce a substantial disruption to water structure, and it is clear the nature of the anion has a significant impact on this structure breaking role of the cation.

Differences between the present chloride solutions and the previous hydroxide solutions can be attributed to the different anions involved. The peculiarities of the solvation shell of the OH^- ion are that, as a consequence of its charge distribution, it forms four strong hydrogen bonds between its oxygen and the surrounding water molecules. The Cl ions instead, both in these salt solutions and in HCl solutions,[11] can be accommodated without dramatic distortions to the water network: it can indeed

substitute an oxygen site with only small differences between the O−Cl−O versus the O−O−O angle distributions. In summary, the distortions to the microscopic structure of water is the result of the combined effect of the cation−anion pair, thus washing out any significance of the definition of "structure maker/breaker" referred to a single ion.

Acknowledgment. This work has been performed within the Agreement No. 01/9001 between CCLRC and CNR, concerning collaboration in scientific research at the spallation neutron source ISIS and with partial financial support of CNR.

References and Notes

(1) Wimby, J.; Berntsson, T. S. *J. Chem. Eng. Data* **1994**, *39*, 68.
(2) Morgan, B.; Madden, P. A. *J. Chem. Phys.* **2004**, *120*, 1402.
(3) MacKinnon, R. Nobel Lecture, December 8, 2003; Morais-Cabral, J. H.; Zhouh, Y.; MacKinnon, R. *Nature* **2001**, *414*, 37.
(4) Hofmeister, F. *Arch. Exp. Path. Pharmakol.* **1888**, *24*, 247.
(5) Bernal, J. D.; Fowler, R. H. *J. Chem. Phys.* **1933**, *1*, 515.
(6) Desnoyers, J. E.; Verral, R. E.; Conway, B. E. *J. Chem. Phys.* **1965**, *43*, 243.
(7) Cox, W. M.; Wolfenden, J. H. *Proc. R. Soc.* **1934**, A 145, 486.
(8) Collins, K. D. *Methods* **2004**, *34*, 300.
(9) Botti, A.; Bruni, F.; Imberti, S.; Ricci, M. A.; Soper, A. K. *J. Chem. Phys.* **2004**, *120*, 10154.
(10) Imberti, S.; Botti, A.; Bruni, F.; Cappa, G.; Ricci, M. A.; Soper, A. K. *J. Chem. Phys.* **2005**, *122*, 194509.
(11) Botti, A.; Bruni, F.; Imberti, S.; Ricci, M. A.; Soper, A. K. *J. Chem. Phys.* **2004**, *121*, 7840.
(12) Hulme, E. C.; Soper, A. K.; McLain, S. E.; Finney, J. L. *Biophys.* **2006**, *91*, 2371.
(13) McLain, S. E.; Soper, A. K.; Watts, A. *J. Phys. Chem.* **2006**, *110*, 21251.
(14) Neilson, G. W.; Enderby, J. E. *Proc. R. Soc. London Ser. A* **1983**, *390*, 353.
(15) Herdman, G. J.; Neilson, G. W. *J. Mol. Liq.* **1990**, *46*, 165.
(16) Ohtaki, H.; Radnai, T. *Chem. Rev.* **1993**, *93*, 1147.
(17) Mancinelli, R.; Botti, A.; Bruni, F.; Ricci, M. A.; Soper, A. K. *Phys. Chem. Chem. Phys.* **2007**, *9*, 2959.
(18) Soper, A. K. *J. Chem. Phys.* **1994**, *101*, 6888.
(19) Soper, A. K. *Chem. Phys.* **1996**, *202*, 295; Soper, A. K. *J. Mol. Liq.* **1998**, *78*, 179; Soper, A. K. *Chem. Phys.* **2000**, *258*, 121; Soper, A. K. *Molec. Phys.* **2001**, *99*, 1503.
(20) Soper, A. K. *Phys. Rev. B* **2005**, *72*, 104204.
(21) In the following the superscript + and −, referring to the charge of the individual ions, will be omitted to make text easier to read.
(22) Postorino, P.; Tromp, R. H.; Ricci, M. A.; Soper, A. K.; Neilson, G. W. *Nature* **1993**, *366*, 668.
(23) Soper, A. K.; Ricci, M. A. *Phys. Rev. Lett.* **2000**, *84*, 2881.
(24) Sears, V. F. *Neutron News* **1992**, *3*, 26.
(25) Egelstaff, P. A. In *Methods of Experimental Physics, Neutron Scattering*; Price, D. L., Skold, K., Eds.; Academic Press: New York, 1987; Vol. 23, Part B, p 405.
(26) see: www.isis.rl.ac.uk/disordered/Sandals/ATLAS manual DTB.pdf.
(27) Soper, A. K. In *Methods in the Determination of Partial Structure Factors*; Suck, J. B., Raoux, D., Chieux, P., Riekel, K. C., Eds.; World Scientific: Singapore, 1993; p 58. Soper, A. K.; Turner, J. Z. *Int. J. Mod. Phys. B* **1993**, *7*, 3049.
(28) McGreevy, R. L.; Howe, M. A. *Ann. Rev. Mat. Sci.* **1992**, *22*, 217.
(29) McGreevy, R. L. *J. Phys. Condens. Matter* **2001**, *13*, R877.
(30) Soper, A. K. In *Proceedings of the Conference on Advanced Neutron Sources 1988*; Hyer, D. K., Ed.; Institute of Physics and Physical Society, London, 1989; IOP Conf. Proc. No. 97 p 353. Detailed information on the SANDALS diffractometer can be also found at the web site: www.isis.rl.ac.uk.
(31) www.isis.rl.ac.uk.
(32) Gee, R. L.; Wallace, W. J.; Raiczak, R. D. *J. Chem. Eng. Data* **1983**, *28*, 305.
(33) Berendsen, H. J. C.; Grigera, J. R.; Straatsma, T. P. *J. Phys. Chem.* **1987**, *91*, 6269.
(34) Enderby, J. E. *Chem. Soc. Rev.* **1995**, *24*, 159.
(35) Impey, R. W.; Madden, P. A.; McDonald, I. R. *J. Phys. Chem.* **1983**, *87*, 5071.
(36) Ramaniah, L. M.; Bernasconi, M.; Parrinello, M. *J. Chem. Phys.* **1999**, *111*, 1587.
(37) Neilson, G. W.; Skipper, N. *Chem. Phys. Lett.* **1985**, *114*, 35.
(38) Laage, D.; Hynes, J. T. *Proc. Natl. Acad. Sci. U.S.A.* **2007**, *104*, 11167.
(39) Ohtaki, H.; Fukushima, N. *J. Sol. Chem.* **2004**, *21*, 23.
(40) Soper, A. K.; Neilson, G. W.; Enderby, J. E.; Howe, R. A. *J. Phys. C* **1977**, 1977, *10*, 1793.
(41) McLain, S. E.; Imberti, S.; Soper, A. K.; Botti, A.; Bruni, F.; Ricci, M. A. *Phys. Rev. B* **2006**, *74*, 094201.
(42) Soper, A. K; Weckström, K. *Biophys. Chem.* **2006**, *124*, 180.